New Apparatus for the Fast Determination of High-Pressure Vapor−Liquid Equilibria of Mixtures and of Accurate Critical Pressures

Luis A. Galicia-Luna* and A. Ortega-Rodriguez

Instituto Politecnico Nacional, Laboratorio de Termodinamica-Graduados-ESIQIE, Edif. Z, Secc. 6, 1ER Piso, UPALM, C.P. 07738, Mexico

D. Richon

Ecole Nationale Supérieure des Mines de Paris, CEREP, Laboratoire de Thermodynamique, 35, Rue Saint-Honoré, 77305 Fontainebleau, France

An apparatus based on the static-analytic method has been designed to perform fast determinations of vapor−liquid equilibria and critical pressures for mixtures up to 60 MPa and 523 K. Vapor pressures of isobutane and vapor−liquid equilibria of the following mixtures—carbon dioxide + ethanol at (312.82, 313.15, 333.82, 333.75, 348.4, and 373.00) K up to 14.3 MPa and carbon dioxide + 2-propanol at (324.99, 324.70, 333.70, 333.82, and 348.65) K up to 10.5 MPa—are reported herein over the whole range of compositions. The experimental data are represented/predicted using the Patel−Teja equation of state (EOS) with new Wong−Sandler type mixing rules. For the carbon dioxide + ethanol and carbon dioxide +2-propanol mixtures, the parameters of the EOS were fitted to the VLE data at 313.15 K and at 324.70 K, respectively. VLE data at higher temperatures were then predicted and found to be in good agreement with the data reported in this work. Critical pressures and compositions were also determined for the system carbon dioxide + ethanol at 312.82, 333.75, 333.82, 348.40, and 373.00 K; all of them are in agreement with those published in the literature.

Introduction

Extraction using supercritical fluids is now being used by industry (Saito and Arai, 1997). However, the design of this type of process requires the knowledge of phase equilibrium diagrams over a large range of temperatures and pressures. The development of supercritical fluid extraction is often strongly dependent on new thermodynamic data including vapor−liquid, liquid−liquid, and vapor−liquid−liquid equilibria. For these purposes, an apparatus has been especially designed and built up, to study one-, two- and three-phase systems composed of either binary or ternary mixtures up to 60 MPa and 523.15 K. Generally, this new apparatus, based on the static-analytic method (Laugier et al., 1986), involves a sampling-analyzing process for determining phase compositions. It has been manufactured by ARMINES-Ecole des Mines and custom designed in the Laboratoire de Thermodynamique de l'Ecole des Mines de Paris for the laboratory of Thermodynamics of The Chemical Engineering School at the Instituto Politécnico Nacional of Mexico.

Regarding the design of the high-pressure equipment, its advantages and original characteristics make it very practical and accurate for the measurements. Only 2 days are required to obtain an isotherm defined by eight pressures for pure compounds and mixtures (sixteen compositions), with uncertainties within 1% at any composition.

* To whom correspondence should be addressed. E-mail: lgalicia@andromeda.esiqie.ipn.mx or lagalicia@dsi.com.mx. Telephone: (52) 5729-6000, ext 55133. Fax: (52) 5586-2728.

The binary systems studied in this work constitute the first set of experimental data as a part of a project currently under way at the Thermodynamics Laboratory of the E.S.I.Q.I.E. (Instituto Politécnico Nacional of Mexico). The main objective of this project is to perform systematic studies of *PVT* data and phase equilibria (Galicia-Luna et al., 1998) of binary mixtures containing CO_2 and alcohols (from ethanol to decanol) in order to select the best supercritical operating conditions for industrial applications such as the extraction of red colorants from *beta vulgaris* and yellow colors of the cempasuchil flour of Mexico (*tagetes erecta*).

Experimental Method and Apparatus

The apparatus is based on the static-analytic method, allowing the analysis of the multiphase equilibrium of binary and multicomponent systems. In this work, the uncertainties of the measurements are typically within ±0.03 K and ±0.02 MPa, and those of the compositions are <1%.

Principle of operation. Vapor−liquid equilibrium conditions are produced inside a thermoregulated equilibrium cell of very simple shape. The equilibrium chamber is stirred efficiently using a magnetic rod driven by an external rotating magnetic field. The equipment uses a compressed air-monitored sampler injector, for extracting and injecting phase samples into the carrier gas circuit of a gas chromatograph. This capillary sampler injector is movable vertically, at about 2 cm/min using a step motor, to immerse the extremity of the capillary inside the phase to be sampled. The equilibrium cell windows allow observ-

10.1021/je990187d CCC: $19.00
Published on Web 01/12/2000

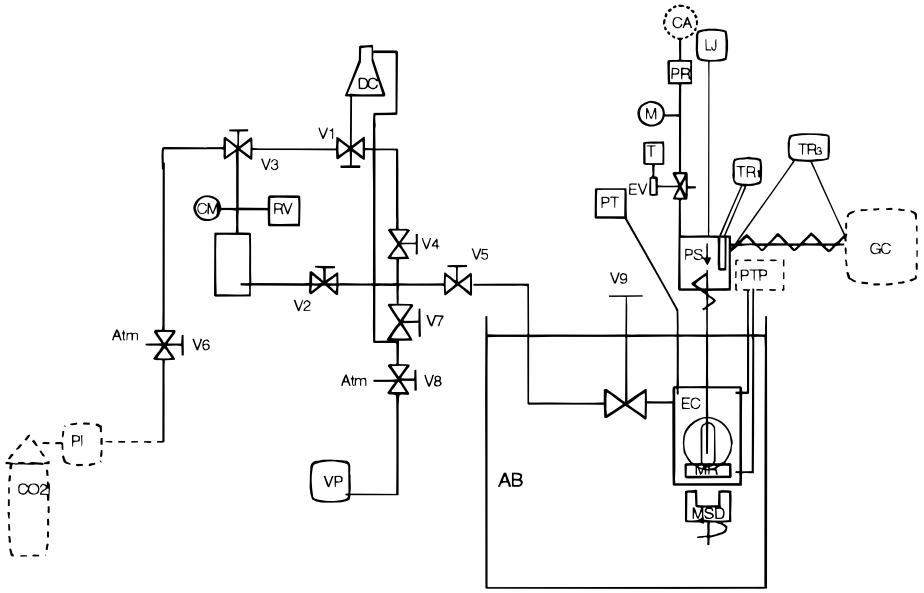

Figure 1. Flow diagram of the apparatus: AB, air bath; CA, compressed air; CM, contact manometer; CO_2, cylinder; DC, degassing cell; EC, equilibrium cell; EV, electrovalve; GC, gas chromatograph; LJ, lifting jack; M, manometer; MR, magnetic rod; MSD, magnetic stirring device; RV, relief valve; PI, Isco pump; PT, pressure transducer; PTP, platinum temperature probe; PR, pressure regulator; PS, phase sampler; T, timer; TR, thermal regulator; V*i*, shut-off valve *i*; VP, vacuum pump.

ing and following the position of the capillary. For pressures and temperatures lying between the defined limits of use, the phase compositions are determined without any disturbance of equilibrium, as they are done on withdrawn samples generally much smaller than 1 mg. The fast transfer of the totality of samples from the equilibrium chamber up to the column of the chromatograph ensures reliability.

Description of the Apparatus. The apparatus consists of the following: the equilibrium cell, the sampler injector, temperature regulators, pressure and temperature measurement systems, the timer and compressed-air control device of the sampler, a magnetic stirring device, and feeding and degassing circuits.

The equilibrium cell (Figures 1 and 2) is composed of a body, EC, on which is fixed a cap, C. The cell body and the cap are both made of stainless steel. The cap has a connection tubing to the pressure transducer, PT. The internal volume of the cell is about 40 cm^3. The magnetic rod, MR, at the bottom of the cell's body is driven from the outside by a rotating magnetic field, the rotation speed of which is controlled with a variable-speed motor.

A movable capillary, MC, goes through C from the sampler to the inner part of the cell, the sealing being achieved with a polymer O-ring. The path of the movable stem closing the extremity of the capillary is adjusted by a differential screw. This path controls the pressure drop at the capillary exit and then the amount of withdrawn sample for a given period of opening time. The opening time, monitored with an electronic timer (Crouzet), is consistent with gas chromatograph analyses, that is, between 0.05 and 1 s. The capillary extends only a short distance outside of the equilibrium cell, thus ensuring a small internal volume compared to that of the withdrawn samples. A heating resistance is used to heat the expansion chamber of the sampler injector in order to have liquid samples vaporized rapidly for good chromatographic analyses.

Two thermometric wells (top and bottom of the cell) drilled in the cell's body receive two platinum temperature probes (100 Ω/0 °C), PTP.

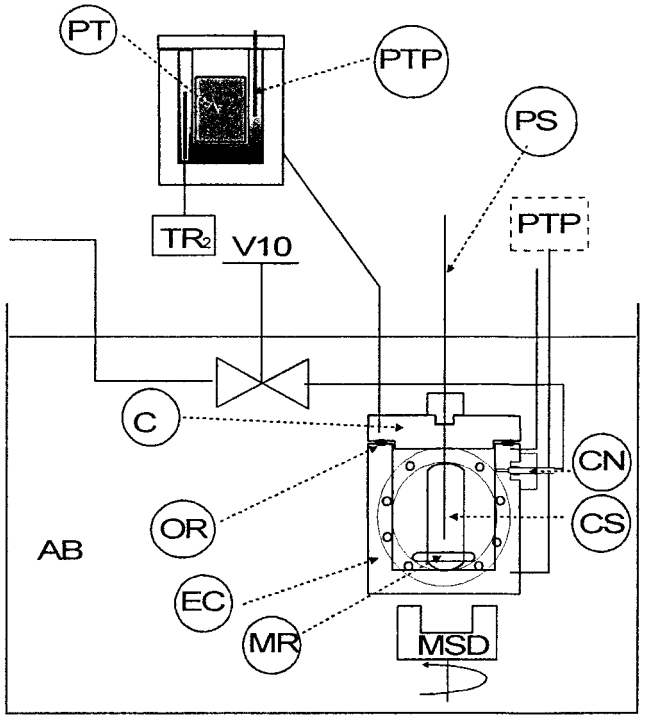

Figure 2. Flow diagram of the equilibrium cell: AB, air bath; C, cap; CN, connecting nut; EC, equilibrium cell; MC, movable capillary; MR, magnetic rod; MSD, magnetic stirring device; OR, O-ring; PS, phase sampler; PT, pressure transducer; PTP, platinum temperature probe; TR*i*, thermal regulator *i*; V*i*, shut-off valve *i*.

Two sapphire windows, sealed by means of viton O-rings, are fixed on opposite sides of the cell's body with stainless steel covers. The whole usable height of the inner part of the cell is visible from outside.

The loading valve V9 is connected to the body of the cell by the connecting nut, CN.

The pressure measurements are made by means of a pressure transducer (Entran 500 EPNM-HT500A) maintained at a specific temperature.

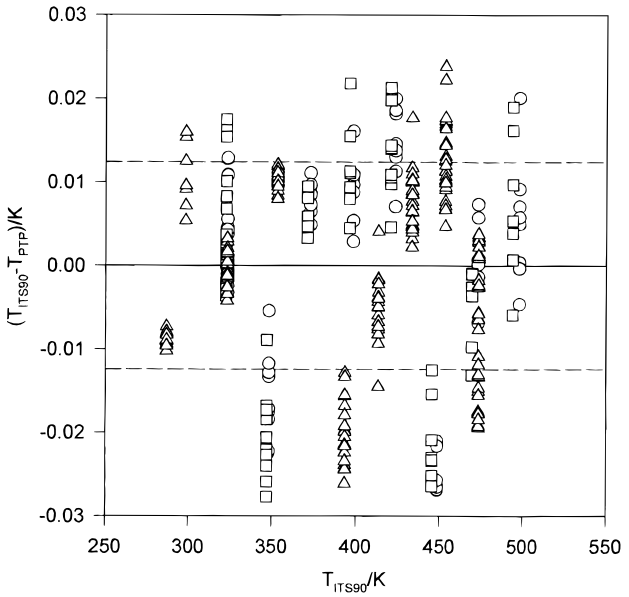

Figure 3. Results of the calibration (second-order polynomial regression) of a platinum probe, $T_{ITS90} - T_{cal}$. over a period of 6 months: ○, Jan. 15, 1998; △, April 10, 1998; □, June 15, 1998; − − −, standard deviation.

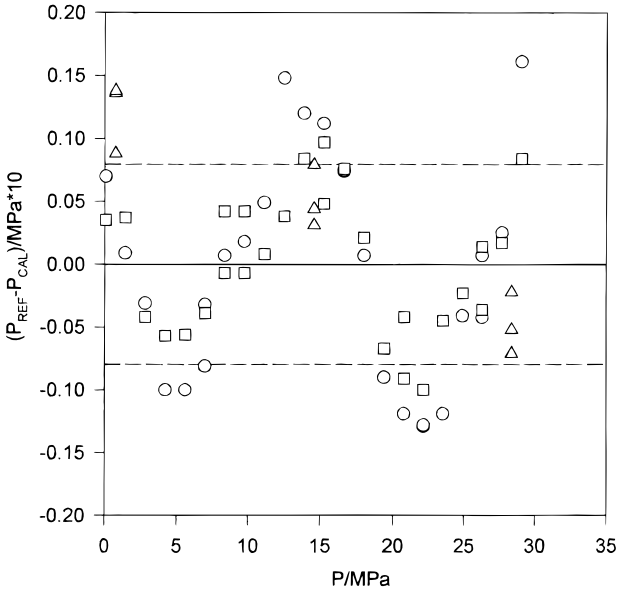

Figure 4. Results of calibration (second-order polynomial regression) of the Entran pressure transducer maintained at a constant temperature of 398.15 K: (− − −) standard deviation.

The temperature of the equilibrium cell is regulated by air bath AB. The temperatures of the phase sampler, PS, and of the pressure transducer, PT, are regulated with West 6100 regulators, TR_1 and TR_2, fitted with thermocouples and heating resistances.

The transferring circuit between the sampler and the gas chromatograph, GC, is heated by means of a linear resistor coupled to a West 6100 regulator, TR_3. The gas chromatograph uses a thermal conductivity detector, TCD, and a 183 cm long and 0.318 cm diameter column packed with Porapack Q 100/120. The GC carrier gas is helium at a flow rate of 30 mL/min, the column temperature is 433.15 K, and those of the injector and of the detector are respectively 433.15 and 463.15 K.

Experimental Procedure. The procedure consists of four steps (see Figure 2): 1, sensors and detector calibrations; 2, cell loading; 3, setting up the experimental conditions; 4, measurements at equilibrium.

The platinum probes (Specitec) connected to digital indicators (Automatic Systems AS-F250 are calibrated against the calibration system F300S fitted with a 25 Ω reference probe (Rosemount, model 162CE) of ±0.005 K certified accuracy traceable to NIST. The uncertainty for both platinum probes is estimated to be ± 0.03 K; see Figure 3. This figure, which presents calibrations over a period of 6 months, indicates a very good time stability of the platinum probe characteristics.

The Entran pressure transducer connected to a $^1/_2$ digital multimeter (HP-34401A) is calibrated at 398.15 K with a DH 5304 dead weight tester (accuracy: ±0.005% full scale). This temperature was selected after testing the pressure transducer at different temperatures from 298 to 473 K. The final accuracy of the measured pressures is about ±0.02 MPa. Figure 4 shows different calibrations over a period of 6 months; the response of the pressure transducer appears stable with time. The calibration of the thermal conductivity detector for CO_2, ethanol, and 2-propanol is achieved by injecting known amounts of the pure compounds through calibrated syringes. Calibration data are fitted to quadratic polynomials, leading to an estimated mole fraction uncertainty <1%.

The liquid component of the mixture to be studied is introduced into the degassing cell, DC, and then degassed (efficient stirring under a vacuum) by activating the vacuum pump, VP (all the valves, except valve 6, are opened to evacuate simultaneously the cell and the whole circuit). After 10 min of degassing the circuit, valves 7 and 1 are closed. Then, the liquid, inside the degassing cell, is vigorously stirred with a magnetic rod during the whole degassing process. After complete degassing, valves 3, 2, 7, and 8 are closed while valves 1, 4, 5, and 9 are opened; the degassing cell is then rotated to let a given quantity of liquid component flow down by gravity into the equilibrium cell.

Valves 1 and 4 are closed while valves 3 and 2 are opened. The lighter (gas or condensable such as CO_2) component is introduced from a 100 MPa (Nova Swiss) gas compressor or an Isco syringe pump (100DM) into the equilibrium cell to set the pressure to its desired value; then, valves 2 and 3 are closed.

Then, the magnetic stirring device, MSD, under the equilibrium cell is activated to drive the magnetic rod, MR, contained inside the equilibrium chamber. The temperatures at the top and bottom of the equilibrium cell are read periodically. When thermal equilibrium is reached (both temperatures are the same within experimental accuracy, and total pressure is constant), the equipment is ready for measurements. Normally, it takes 20 min to reach equilibrium conditions.

Samples of liquid and vapor are withdrawn and analyzed. At a given temperature and pressure, we normally work on at least five samples of each phase in order to check for the repeatability and perform vapor mole fraction error analyses.

Isothermal phase envelopes are obtained by consecutive pressure increments.

Modeling. The binary VLE was done with the Patel−Teja equation of state (PT-EoS):

$$P = \frac{RT}{v-b} - \frac{a[T]}{v(v-b)+c(v-b)} \qquad (1)$$

In this equation, the critical compressibility factor (ζ_c) is treated as an empirical constant and the pure component

parameters a, b, and c are given by the following equations:

$$a[T] = \Omega_a\left(\frac{R^2 T_c^{\,2}}{P_c}\right)\psi[T_R] \tag{2}$$

$$b = \Omega_b\left(\frac{RT_c}{P_c}\right) \tag{3}$$

$$c = \Omega_c\left(\frac{RT_c}{P_c}\right) \tag{4}$$

where:

$$\Omega_c = 1 - 3\zeta_c \tag{5}$$

$$\Omega_a = 3\xi_c^{\,2} + 3(1 - 2\zeta_c)\Omega_b + \Omega_b^{\,2} + 1 - 3\zeta_c \tag{6}$$

and Ω_b is the smallest positive root of:

$$\Omega_b^{\,3} + (2 - 3\zeta_c)\Omega_b^{\,2} + 3\zeta_c^{\,2}\Omega_b - \zeta_c^{\,3} = 0 \tag{7}$$

The temperature dependence of $\psi[T_R]$ is defined in a similar way as in the Soave (1972) and Peng−Robinson (1976) equations of state:

$$\psi[T_R] = [1 + F(1 - T_R^{\,1/2})]^2 \tag{8}$$

where:

$$F = 0.452\,413 + 1.309\,82\omega - 0.295\,937\omega^2 \tag{9}$$

And the critical compressibility factor is given as a function of the acentric factor:

$$\zeta_c = 0.329\,032 - 0.076\,799\omega + 0.021\,194\,7\omega^2 \tag{10}$$

The mixing rules for the PT-EOS proposed by Galicia-Luna et al. (1999) are given by:

$$\frac{a}{RT} = \frac{(3b + c)}{2}D \tag{11}$$

$$b = \frac{2Q + cD}{2 - 3D} \tag{12}$$

$$c = \sum_i x_i c_i \tag{13}$$

In eq 12 we used the combination rule (Wong and Sandler, 1992)

$$B_{ij}(T) = \left(b - \frac{a}{RT}\right)_{ij} = \frac{1}{2}\left[\left(b_i - \frac{a_i}{RT}\right) + \left(b_j - \frac{a_j}{RT}\right)\right](1 - k_{ij}) \tag{14}$$

where

$$D = \sum_i \frac{x_i a_i}{RT}\ln\left(\frac{2}{3b_i + c_i}\right) - \frac{G_\gamma^{ex}}{RT} \tag{15}$$

$$Q = \sum_i\sum_j x_i x_j\left(b - \frac{a}{RT}\right)_{ij} \tag{16}$$

The activity coefficient model used in eq 15 is the NRTL model (Renon and Prausnitz, 1968):

$$G_\gamma^{ex} = \sum_i x_i \frac{\sum_j \tau_{ji} g_{ji} x_j}{\sum_k g_{ki} x_k} \tag{17}$$

$$\tau_{ij} = \frac{\delta_{ij}}{RT} \tag{18}$$

$$g_{ij} = \exp(-\alpha_{ij}\tau_{ij}) \tag{19}$$

Results and Discussions

The purity and origin of chemicals used in this work are given in Table 1. They were used without any purification except for a careful degassing of ethanol and 2-propanol.

Literature data sources are given in Table 2. Our VLE experimental results are given in Tables 3 and 4 for respectively the carbon dioxide + ethanol and carbon dioxide + 2-propanol binary systems.

The vapor pressure of isobutane has been determined from 317.72 to 406.97 K; the results are compared to those published by Waxman and Gallagher (1983), and the deviations between the two data sets do not exceed ±0.08 MPa. Before comparison, the data from Waxman and Gallagher (1983) were converted to the ITS90 temperature scale.

Waxman and Gallagher (1983) fitted their data with the following polynomial equation:

$$P_{vap} = P_c^* \exp\left[\frac{T_c}{T}\left(E_1\left(1 - \frac{T}{T_c}\right) + E_2\left(1 - \frac{T}{T_c}\right)^{3/2} + E_5\left(1 - \frac{T}{T_c}\right)^3\right)\right] \tag{20}$$

Our vapor pressures are given in Table 2. Figure 5 presents the deviations $P_{vap} - P_{poly}$. A pressure transducer (Sedeme 40 MPa) was used for these purposes; it has an estimated uncertainty of less than ±0.008 MPa.

The carbon dioxide + ethanol system at 313 K was chosen as the test system over the whole range of compositions (see Figure 6), to test the equipment by making reliable comparisons of data from this work and the literature. VLE data for the carbon dioxide + ethanol system have been determined, within the whole range of compositions at 313.15 K in Ecole des Mines (Fontainebleau) and at 312.82 K in Instituto Politecnico Nacional (Mexico). Both sets of equipment are based on a static-analytic method. Both sets of data are in excellent agreement. The VLE data at 313.15 K were fit to the PT-EoS (1986) with the new mixing rules recently developed by Galicia-Luna et al. (1999).

The parameters fitted for the NRTL model are τ_{ij}, α_{ij}, and k_{ij} (see eq 14). The pure-component parameters (T_c, P_c, and ω) for the PT-EoS used here are those given by Reid et al. (1986). The VLE calculation algorithm was use in combination with the Marquardt−Lebenberg method (IMSL, 1979) with the objective function

$$F = \sum_{j=1}^{Nd}\left[\sum_{i=1}^{Nc}\left(\frac{y_{ij}^{calc} - y_{ij}^{exp}}{y_{ij}^{exp}}\right)^2 + \left(\frac{P_j^{cal} - P_j^{exp}}{P_j^{exp}}\right)^2\right] \tag{21}$$

The optimized parameters for the PT-EoS with the NRTL mixing rule at 313.15 K for the system CO_2 (1) + ethanol (2) are $\alpha_{ij} = 0.401$, τ_{12} (J/mol) = 112.8251, τ_{21} (J/mol) = 0.81219, and $k_{12} = 0.4188$.

These sets of parameters were used to predict the vapor−liquid equilibria at 312.82 K. Comparisons with data

Table 1. Purity and Origin of Pure Compounds

compound	certified purity (%)	max. water content (%)	supplier
ethanol	99.8	0.02	Merck
2-propanol	99.7	0.05	Baker
CO_2	99.995		Air Products−Infra
helium	99.995		Air Products−Infra
isobutane	99.97		

Table 2. Selected Papers for the CO_2 + Ethanol System

	range		indicated purity (%)	
ref	*T*/K	*P*/MPa	CO_2	ethanol
Gurdial et al. (1993)	305.8−325.1	7.65−9.74	99.8	99.8
Suzuki et al. (1990)	313.4−338.4	0.514−10.654	99.99	99.5
Yoon et al. (1993)	313.2	0.6−8.15	99.9	99.5

Table 3. Vapor−Liquid Equilibrium Data for the System Carbon Dioxide (1)/Ethanol (2) at Different Temperatures

P/MPa	x_1	y_1	*P*/MPa	x_1	y_1
T = 312.82 K[a]			T = 313.15 K[b]		
1.664	0.1006	0.9854	0.476	0.0237	0.9520
3.109	0.1914	0.9888	0.520	0.0267	0.9605
5.421	0.3676	0.9904	1.301	0.0729	0.9798
6.983	0.5303	0.9885	2.204	0.1296	0.9849
8.120	0.9459	0.9784	3.092	0.1862	0.9884
8.154	0.9669	CP	4.196	0.2656	0.9910
			5.196	0.3408	0.9905
			6.237	0.4401	0.9901
			7.468	0.6669	0.9871
T = 333.82 K[a]			T = 333.75 K[b]		
0.931	0.0344	0.9335	3.069	0.1277	0.9708
2.382	0.1032	0.9721	8.342	0.4530	0.9702
3.044	0.1373	0.9759	10.626	0.7787	0.9154
5.272	0.2435	0.9815	10.703	0.8120	0.9049
4.458	0.2038	0.9806	10.760	0.8562	CP
6.210	0.2992	0.9818			
7.096	0.3536	0.9810			
9.188	0.5208	0.9677			
10.485	0.7151	0.9293			
10.803	0.7951	0.8962			
10.842	0.8231	0.8476			
10.878	0.8323	CP			
T = 348.40 K[a]			T = 373.00 K[a]		
1.515	0.0576	0.9176	2.176	0.0649	0.8827
3.515	0.1391	0.9606	4.220	0.1350	0.9165
5.518	0.2213	0.9618	6.151	0.2054	0.9328
7.634	0.3285	0.9599	9.165	0.3358	0.9161
10.607	0.5193	0.9425	12.024	0.4790	0.9120
12.002	0.6718	0.9003	12.821	0.5303	0.8980
12.301	0.7273	0.8851	14.114	0.6593	0.8297
12.460	0.7980	C.P.	14.345	0.7181	CP

[a] Measurements done at IPN. [b] Measurements done at Ecole des Mines de Paris.

reported by Suzuki et al. (1990) show good agreement (Figure 6). The error percentage and the standard deviation for the vapor pressure and the vapor-phase composition are given in Table 6.

The two isotherms at 333.82 K and 333.75 K are in good agreement (see Table 6) with the data published by Suzuki et al. (1990), as shown in Figure 7. All experimental data determined in this work for the carbon dioxide + ethanol system are reported in Table 3.

PTxy data for the carbon dioxide + 2-propanol system are given in Table 4 and displayed in Figure 8. VLE data are reported at 314 K and 335 K for this system by Radosz et al. (1986); they were obtained via a dynamic method using carbon dioxide. From Figure 8, there is a clear

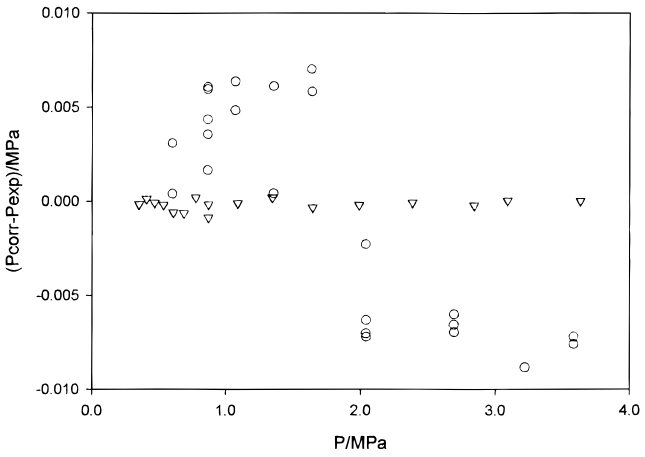

Figure 5. Comparison of saturated vapor pressure: ○. this work; ▽, Waxman and Gallagher.

Table 4. Vapor−Liquid Equilibrium Data for the System Carbon Dioxide(1)/2-Propanol (2)

P/MPa	x_1	y_1	*P*/MPa	x_1	y_1
T = 324.70 K			T = 324.99 K		
1.555	0.0504	0.9721	1.640	0.0615	0.9732
3.281	0.1297	0.9809	3.478	0.1464	0.9749
4.927	0.2361	0.9764	5.118	0.2417	0.9819
6.144	0.3155	0.9770	7.128	0.4166	0.9777
7.133	0.4125	0.9789	8.520	0.6105	0.9695
8.052	0.5215	0.9760	9.180	0.7977	0.9483
8.508	0.6007	0.9746			
8.905	0.7108	0.9706			
T = 333.70 K			T = 333.82 K		
1.751	0.0603	0.9450	1.025	0.0358	0.9371
3.136	0.1265	0.9707	3.084	0.1192	0.9715
4.188	0.1761	0.9747	5.139	0.2181	0.9699
6.053	0.2801	0.9725	6.971	0.3373	0.9684
6.988	0.3398	0.9715	8.151	0.4329	0.9664
5.140	0.2284	0.9748			
7.572	0.3859	0.9721			
8.065	0.4291	0.9691			
8.777	0.5121	0.9640			
9.447	0.6130	0.9582			
T = 348.60 K					
1.752	0.0573	0.9257			
4.061	0.1387	0.9488			
6.024	0.2301	0.9567			
8.023	0.3517	0.9512			
10.448	0.5721	0.9266			

disagreement between our data and those published by Radosz et al. (1986). For this reason we determined two sets of data at 333.70 K and 333.82 K with different chromatograph conditions, with no influence of them on the final results. The VLE data at 324.70 K were fitted to the PT-EoS (1986) with the new mixing rules, and the optimized parameters for the system carbon dioxide + 2-propanol are $\alpha_{ij} = 0.350$, τ_{12} (J/mol) = 121.3830, τ_{21} (J/mol) = 65.2578, and $k_{12} = 0.5153$. The error percentage and the standard deviation for the vapor pressure and the vapor-phase composition are given in Table 7. Our experimental data are well represented by the model (see Table 7).

Critical points. The critical properties (P_c, T_c, z_c) are obtained with the same accuracy as that for vapor−liquid equilibria by gas chromatograph analyses coupled to direct visual observation through the sapphire windows. The shapes of the phase envelopes near the critical points are in good agreement with these critical points for all of the five temperatures at which the carbon dioxide + ethanol system has been studied.

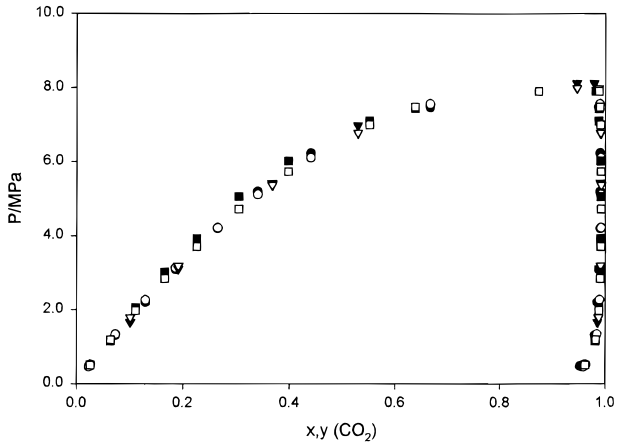

Figure 6. Vapor liquid equilibrium data for the carbon dioxide + ethanol system: ▽, this work (IPN) at 312.82 K; ■, Suzuki et al. at 313.4 K; ●, this work (Ecole des Mines de Paris) at 313.15 K; open symbols, calculated/predicted points for the Patel-Teja EOS.

Table 5. Critical *PTx* Data for the System Carbon Dioxide (1)/Ethanol (2)

P/MPa	x_1	*T*/K
8.154	0.9669	312.82
10.760	0.8562	333.75
10.878	0.8323	333.82
12.460	0.7980	348.40
14.345	0.7181	373.00

Table 6. Error Percentage and Standard Deviation for the Vapor Pressure and the Vapor-Phase Composition for the CO_2 (1) + Ethanol (2) System

Modelo G^{ex}	% error P^b	% error $y(1)^b$	STD P	STD $y(1)$	T (K)
NRTL	1.88	0.306	2.23	0.0037	313.15
NRTL	2.32	0.326	2.98	0.0040	323.15 + 312.82
NRTL	2.76	0.268	3.49	0.0034	323.15 + 312.82 + 313.4[b]
NRTL	4.22	0.666	5.38	0.0123	333.4[b]
NRTL	4.28	0.676	5.50	0.0133	333.75 + 333.82 + 333.4

[a] The errors are defined by the following equations

$$\%\ \text{error}\ P = \frac{\sum_{i=1}^{Nd} \left| \frac{P_i^{exp} - P_i^{cal}}{P_i^{exp}} \right|}{Nd} \times 100 \quad \text{and} \quad \%\ \text{error}\ y(1) = \frac{\sum_{i=1}^{Nd} \left| \frac{y_{1i}^{exp} - y_{1i}^{cal}}{y_{1i}^{exp}} \right|}{Nd} \times 100$$

[b] Susuki et al., 1990.

Table 7. Error Percentage and Standard Deviation for the Vapor Pressure and the Vapor-Phase Composition for the CO_2 (1) + 2-propanol (2) System

Modelo G^{ex}	% error P	% error $y(1)$	STD P	STD $y(1)$	T (K)
NRTL	2.61	0.797	3.10	0.0086	324.70
NRTL	5.89	1.61	8.10	0.0285	324.70 + 324.99 + 333.70 +333.82 + 348.60

Experimental measurements of vapor−liquid equilibria near the critical point and of critical loci for binary mixtures (containing carbon dioxide, ethanol, 1-propanol, 1-butanol) are current and will be published later. The overall range of the critical opalescence is less than ±0.02 MPa. The critical mole fractions are determined with repeatability better than ±0.002.

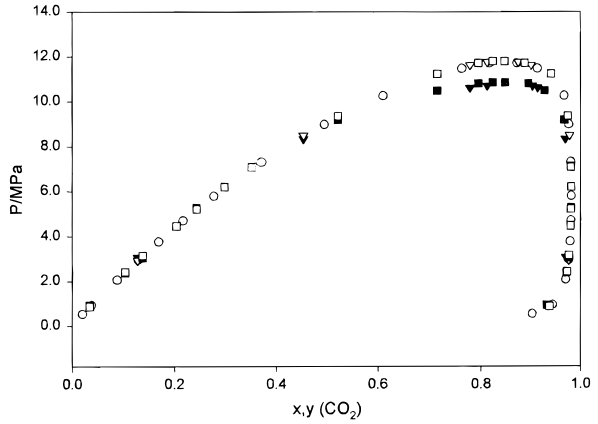

Figure 7. Vapor−liquid equilibrium data for the carbon dioxide−ethanol system: ▼, this work at 333.75 K; ■, this work at 333.82 K; ●, Suzuki et al. (1990) at 333.4 K. The solid symbols are the experimental data reported in this work, and the open symbols are predicted by the Patel-Teja EOS, fitting the parameters at the isotherm at 313.15 K.

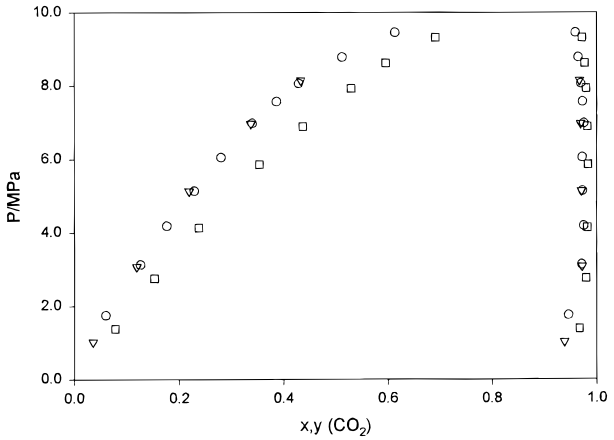

Figure 8. Vapor−liquid equilibria for the carbon dioxide + 2-propanol system: ▽, this work at 333.82 K; ○, this work at 333.70 K; □, Radosz et al. at 335.0 K.

Table 8. Vapor Pressure for Isobutane

T/K	*P*/MPa	*T*/K	*P*/MPa
317.72	0.598	374.53	2.031
317.73	0.601	374.53	2.032
332.87	0.865	374.49	2.034
332.87	0.867	374.49	2.030
332.88	0.868	390.02	2.682
332.89	0.870	390.02	2.683
332.89	0.870	389.99	2.681
342.39	1.074	400.57	3.209
342.40	1.076	400.57	3.209
353.46	1.358	406.97	3.573
353.46	1.353	406.97	3.572
362.87	1.641		
362.99	1.643		

The critical points obtained for the system carbon dioxide + ethanol are reported in Table 5 and presented in Figure 9. Our results are in good agreement with those published by Yoon et al. (1983), Lim et al. (1994), Takashima et al. (1986), and Baker and Anderson (1957). Pressure deviations are about 1% with respect to data published by Gurdial et al. (1993).

Conclusions

A static-analytic apparatus to measure phase equilibria was designed and built. The results presented here demonstrate its ability to achieve reliable vapor pressures of

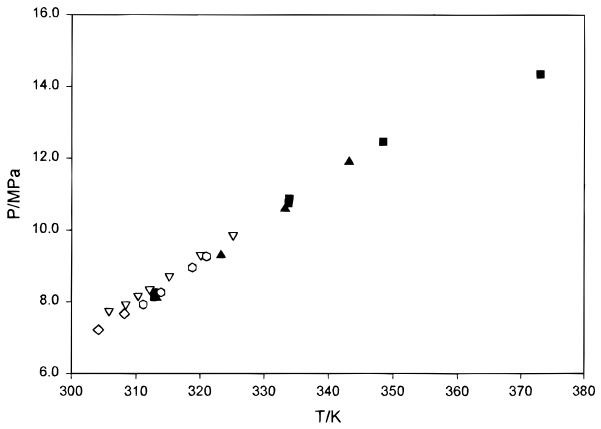

Figure 9. Critical points of the carbon dioxide + ethanol system reported by several authors: ●, Yoon et al., 1993; ▽, Gurdial et al., 1993; ■, this work; ◇, Lim et al., 1994; ▲, Takashima et al., 1986; ○, Baker and Anderson, 1957.

fluids, VLE, and critical points of fluids mixture determinations up to 523 K and 60 MPa. The VLE of the carbon dioxide + ethanol and carbon dioxide + 2-propanol systems and the critical points of the carbon dioxide + ethanol system have been measured and are represented correctly with the Patel−Teja equation of state involving the new mixing rules developed by Galicia-Luna et al., (1999).

Acknowledgment

The authors are grateful to A. Chareton (ENSMP) for its participation in experimental determinations. L.A.G.-L. wants to address special thanks Dr. J. E. Villa-Rivera and Ing. Timoteo Pastrana for their help and encouragement from 1993 to create the first high-pressure thermodynamic laboratory of Mexico.

Literature Cited

Baker, L. C. W.; Anderson, T. F. *J. Am. Chem. Soc.* **1957**, *79*, 2071.

Brunner, G. Industrial Process Development: Countercurrent Multistage Gas Extraction Processes. *Proceedings of the 4th International Symposium on Supercritical Fluids*, Sendai, Japan, May 11−14, 1997; Vol. C, pp 745−756.

Galicia-Luna, L. A.; Escobedo-Alvarado, G. N.; Díaz-Ramirez, N.; A New Mixing Rule for the Patel-Teja Equation of State. Will send to *Ind. Eng. Chem. Res.* 1999.

Gurdial, G. S.; Foster, N. R.; Yun, S. L. J.;Tilly, K. D. Phase behavior of supercritical fluid-entrainer systems. *Supercritical Fluid Engineering Science*; ACM Symposium Series No. 514; American Chemical Society: Washington, DC, 1993; pp 34−45.

IMSL. *The IMSL Library*; IMSL Inc.: Houston, 1979; Vol. 2.

Knapp, H.; Döring, R.; Oellrich, L.; Plöcker, U.; Prausnitz, J. M. *Vapor-Liquid Equilibria for Mixtures of Low boiling Substances*; DECHEMA Chemistry Data Series Vol. VI; Frankfurt, 1982.

Laugier, S.; Richon, D. New apparatus to perfom fast determinations of mixtures vapor-liquid equilibria up to 10 MPa and 423 K. *Rev. Sci. Instrum.* **1986**, *57*, 469−472.

Lim, J. S.; Lee, Y. Y.; Chun, H. S. Phase Equilibria for Carbon Dioxide−Ethanol−Water System at Elevated Pressures. *J. Supercrit. Fluids* **1994**, *7*, 219−230.

Mendoza de la Cruz, J. L.; Ortega-Rodríguez, A.; Galicia-Luna, L. A. Equilibrio liquido-Vapor del sistema CO_2+Etanol a 353.04 K y hasta 10.7 MPa. *Proceedings of the International Symposium of the ESIQIE*, May 27−29, 1998.

Ortega-Rodríguez, A.; Galicia-Luna, L. A. Equilibrio liquido Vapor del sistema CO_2+*n*-Heptano a 353.04 K y hasta 11.6 MPa. *Proceedings of the International Symposium of the ESIQIE*, May 27−29, 1998.

Patel, N. C.; Teja, A. S. A New Cubic Equation of State for Fluids and Fluid Mixtures. *Chem. Eng. Sci.* **1982**, *37*, 463.

Peng, D. Y.; Robinson, D. B. A New Two-Constant Equation of State. *Ind. Eng. Chem. Fundam.* **1976**, *15*, 59.

Radosz, M. Vapor-liquid equilibrium for 2-propanol and carbon dioxide. *J. Chem. Eng. Data* **1986**, *31*, 43−45.

Reid, R. C.; Prausnitz, J. M.; Poling, B. E. *The Properties of Gases & Liquids*. McGraw-Hill: Singapore, 1986.

Renon, H.; Prausnitz, J.-M. Local composition in thermodynamic excess function for liquid mixtures. *AIChE J.* **1968**, *14*, 135−144.

Soave, G. Equilibrium Constants from a Modified Redlich-Kwong Equation of State. *Chem. Eng. Sci.* **1972**, 1197.

Suzuki, K.; Sue, H.; Itou, M.; Smith, R. L.; Inomata, H.; Arai, K.; Saito, S. Isothermal vapor-liquid equilibrium data for binary systems high pressure: carbon dioxide-methanol, carbon dioxide-ethanol, carbon dioxide-1-propanol, methane-ethanol, methane-1-propanol, ethane-ethanol and ethane-1-propanol systems. *J. Chem. Eng. Data* **1990**, *35*, 63−66.

Takishima, S.; Saiki, K.; Arai, K.; Saito, S. J. *J. Chem. Eng. Jpn.* **1986**, *19*, 48.

Waxman, M.; Gallagher, J. S. Thermodynamic properties of isobutane for temperatures from 250 to 600 K and pressures from 0.1 to 40 MPa. *J. Chem. Eng. Data* **1983**, *28*, 224−241.

Wong, D. S. H.; Sandler, S. I. A Theoretically Correct Mixing Rule for Cubic Equations of State. *AIChE J.* **1992**, *38*, 671.

Yoon, J.-H.; Lee, H.-S.; Lee, H. High-Pressure Vapor−Liquid Equilibria for Carbon Dioxide + Methanol, Carbon Dioxide + Ethanol, and Carbon Dioxide + Methanol + Ethanol *J. Chem. Eng. Data* **1993**, *38*, 53−55.

Received for review July 12, 1999. Accepted November 15, 1999. The authors are grateful to CONACYT (project 25432-A), IPN, and his PIFI program for their financial support.

JE990187D